Scanning Electrochemical Microscope Electrode Fabrication

An Undergraduate Honors Thesis

Jacob Maddox

Spring 2016

Presented in Partial Fulfillment of the Requirements for Graduation with Distinction in the Department of Mechanical Engineering at The Ohio State University

Honor's Defense Committee:

Dr. Vishnu Sundaresan – Advisor

Dr. Hanna Cho

This work was supported in part by the College of Engineering and HEKA Elektronik GmbH.

Abstract

Current electrochemical methods subject a sample to an electrical potential and monitor the current to study chemical reactions associated with the reduction-oxidation (redox) reactions. Among electrochemical characterization methods, scanning electrochemical microscopy (SECM) examines the electrochemical behavior at a liquid-solid or liquid-liquid interface. SECM is accomplished via a nanoelectrode which probes the interface and measures the (redox) current in the near field vicinity of the nanoelectrode tip. The redox current measured is not only dependent on the reaction itself, but also varies with the distance between the electrode and sample making it difficult to analyze rough samples. To compensate for topographic variation, shear force (SF) imaging can be used simultaneously to maintain a constant working distance between electrode and sample. The SF imaging technique is applied by attaching two piezoelectric wafers to the nanoelectrode to both induce and measure the amplitude of vibration along the nanoelectrode tip in solution. This vibrational behavior varies in the immediate vicinity of a surface at certain operational frequencies and can be used to directly map distance from a surface to electrical potential experienced by the measuring piezo. Currently, there are limitations to this technique due to structural damping in the electrodes that results from fabrication and limit their sensitivity during SF operation. The purpose of this work was to develop a fabrication technique for SECM nanoelectrodes with less structural dampening for enhanced SF imaging. Failure mode analysis of previously researched fabrication techniques (10% yield) was conducted to determine modifications needed to produce a new method with a predicted 60% yield. Furthermore, the SF amplitude and sensitivity of nanoelectrodes produced using the new method were increased by 250% and 210% respectively on average.

Acknowledgements

I would like to acknowledge HEKA Elektronik GmbH. for their support of this project. Especially Dr. Christian Heinemann, who provided invaluable feedback from start to finish.

I would like to thank my advisor, Dr. Vishnu Baba Sundaresan, for the opportunity to work on this project. The technical and professional guidance he has offered me has been a defining part of my time at OSU and I am incredibly grateful. I would also like to thank Dr. Hanna Cho for serving on my defense committee.

I would also extend my thanks Dr. Robert Northcutt. He has been an exceptional mentor and teacher to me and his contributions were important to my success. Finally, I thank my peers in the lab, especially Hugo van der Walt, who introduced me to research and made it immeasurably more enjoyable.

Table of Contents

List of Figures

List of Tables

Chapter 1: Introduction

1.1 SECM and Electrochemistry

Electrochemistry is the study of the interrelation between electrical and chemical potentials. Current electrochemical techniques typically involve subjecting a sample to an electrical potential and monitoring the chemical reactions associated with the reduction-oxidation (redox) reactions, often through current measurement. Monitoring redox reactions is important for the study of corrosive materials, self-assembled monolayers, polymers, transport through biological tissues, and other fields where electron transfer plays an important role [1]. Conclusions can be drawn about the phenomena taking place by monitoring the transfer of electrons, or current, that occurs through or near a sample [2]. Scanning electrochemical microscopy (SECM) is an experimental technique which enables real time monitoring of the current associated with redox reactions at liquid-solid or liquid-liquid interfaces [3].

A redox reaction is a chemical process by which one species loses an electron through oxidation while another gains an electron through reduction. An important concept for SECM is that when the reaction occurs in a small nanoelectrode tip, there is a diffusion limited process based on the rate at which ions can transport to a metal core [4]. Transfer rates are limited by a geometry in which a planar surface is mostly insulative, with only small portion being conductive and therefore able to participate in redox reactions. Most SECM electrodes are assumed to have mostly insulative disk-shaped tips with a small circular conductive center. The tip of the electrode is assumed to have a hemispherical "diffusion shell" beyond the tip within which it can participate in redox reactions [5]. The electron transfer described, known as the faradaic current, can be measured via an SECM nanoelectrode under one of two modes of operation: Feedback Mode (FB) or Generation Collection (GC) Mode.

In Feedback Mode, the sample is placed in a solution which participates in the reaction known as the redox mediator [6]. As the nanoelectrode is lowered into the liquid, an electrical potential is applied at the tip which drives oxidation of the redox species in the solution. Two stationary electrodes are also required to be present in solution for the reaction to take place: the reference and the counter. The applied potential is set against a reference electrode and the counter electrode serves as a ground. The working electrode is initially in bulk solution and only interacts with the mediator. As the nanoelectrode is brought toward the surface, the faradaic current varies because more of the sample occupies the near field vicinity of the electrode [7]. If the sample surface is inert, the faradaic current will drop because the sample physically blocks interaction between the mediator and electrode tip (Figure 1a). Conversely, an active sample participates in the reaction, and can regenerate the redox species via electrochemical conversion which increases the current measured at the tip (Figure 1b). A schematic of an experimental setup for FB operation is shown in Figure 2.

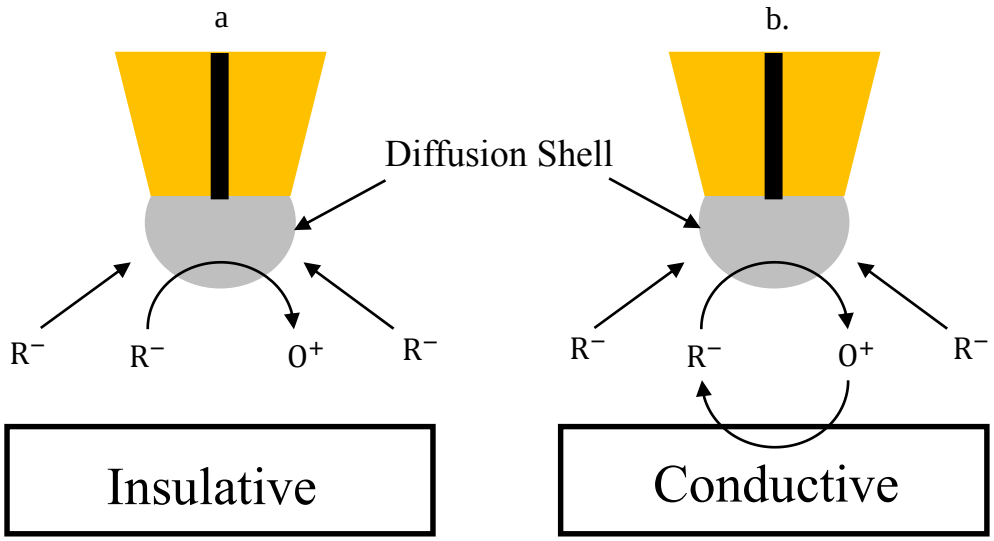

Figure 1: Electrode tip as it reacts with an insulative and conductive sample.

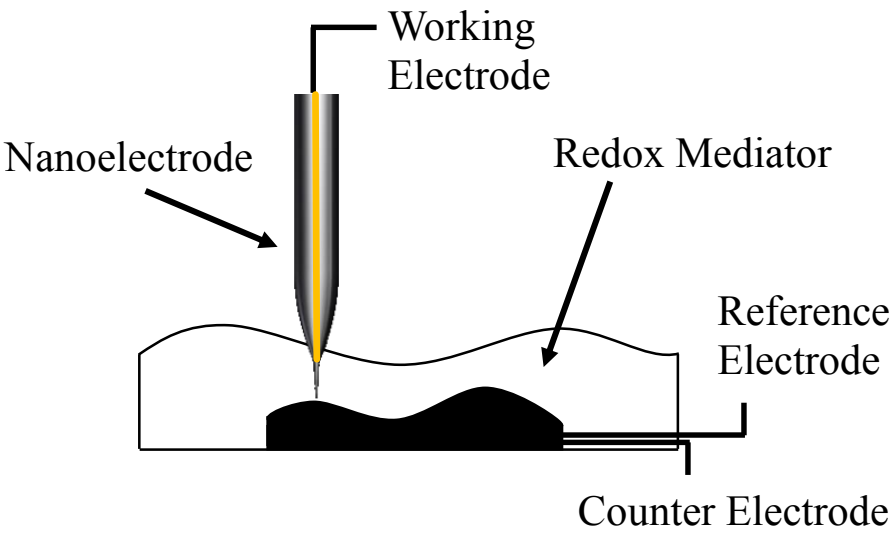

Figure 2: Schematic of experimental setup in FB operation.

GC mode is primarily different in that there is no redox mediator present in the reaction. Instead, the nanoelectrode participates directly with the substrate as it approaches active regions. In GC mode, a potential is applied to the electrode tip which allows it to detect oxidizable or reducible species on the substrate. These species are present on the sample when a separate potential is applied. GC is a more direct measurement of the oxidation or reduction of the sample, and it can sometimes be used in situations when FB operation is not an option. However, drawbacks to using GC mode include inferior spatial resolution and greater time dependency, making FB mode a useful alternative [8].

Under both types of operation, a key component for effective SECM experimentation is the nanoelectrode itself [9]. The size of the hypothetical field of influence directly affects the diffusion limited current and is proportional to the conductive region's size. The effects of the nanoelectrode geometry are consistent across both modes of operation and its properties affect the current measured as described by equation (1) where g is a geometric constant (4 for disks with ~infinitely large insulators), n is the number of electrons transferred per molecule, F is Faraday's

constant, D is the diffusion coefficient, c* is the bulk concentration of the mediator, and r_T is the radius of the conductive part of the nanoelectrode tip [10]. The current in equation (1) specifically refers to the peak to peak current measured in a cyclic voltammogram (CV), where a CV is a type of electrochemical measurement in which a sawtooth potential is applied to the working electrode with the maximum and minimum applied potential being set at values higher than oxidation and lower than reduction reaction potentials of interest, respectively. If the range of applied potentials is large enough, a CV gives information on the anodic and cathodic peak locations (in V) and amplitudes (in A). The difference between the currents measured at the respective potentials is the peak to peak current and can be used with equation (1).

$$\boldsymbol{i_T = gnFDc^* r_T} \qquad (1)$$

Not shown in Equation (1) is the measured current's dependence on the distance between the nanoelectrode tip and sample surface**.** The working distance of the system plays a significant role in current measurement as it determines the degree to which the sample occupies the diffusion shell. Therefore, SECM can be used to measure surface morphology of inert samples. However, if the sample is redox active, the sample must maintain the working distance of the electrode or the current is indistinguishable to distance or redox active areas. To analyze a sample surface, the electrode is moved across the surface. This motion follows one of two profiles: constant height or constant distance. In constant height mode, the electrode is lowered to a fixed z-distance before scanning the sample in the x- and y-directions similar to the 2-D representation in Figure 3. Constant height mode would be very effective if the sample were ideally planar; however, many samples have contours that can result in the sample surface extending beyond the reach of the diffusion shell such that the electrode is no longer sensitive to topographic variation [11]. The

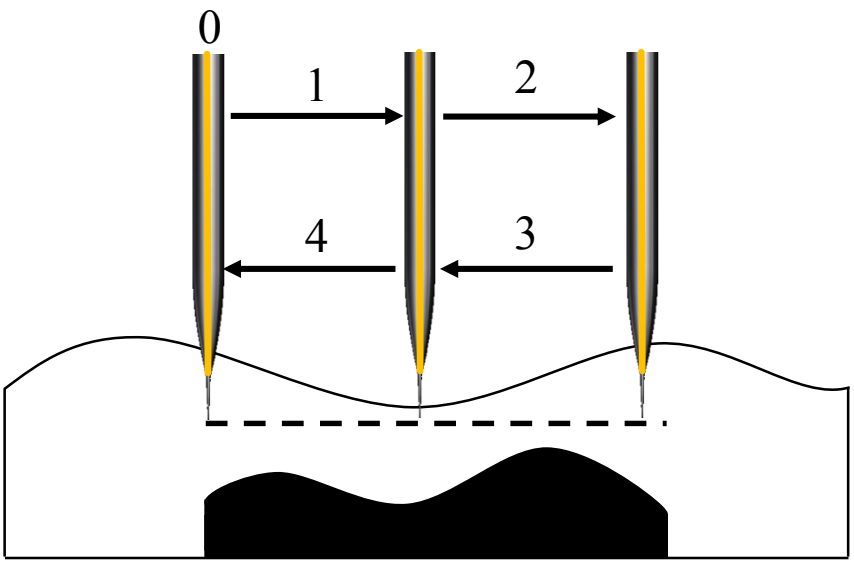

Figure 3: Constant height schematic. The electrode begins at 0 and is moved sequentially as indicated by the arrows.

topography of the sample can more accurately be determined via constant distance mode, represented by Figure 4**.** In constant distance mode the current is continuously measured as the electrode is lowered toward the sample [12]. Due to the current's dependence on the working distance, represented by d, the collected data allows the user to assign a current threshold that corresponds to a specified distance above the sample. As the electrode scans in the x- and y-directions, it is lowered in the z-direction until the threshold is met, the z-position is recorded, and the electrode is raised before moving to the next position. Throughout the scan, the coordinates at which the threshold current occurs is monitored and surface topography is measured. While Constant Distance mode is much slower than Constant Height, it eliminates the possibility of the sample moving out of the range of the diffusion shell and losing sensitivity. However, both methods are only effective for inert samples.

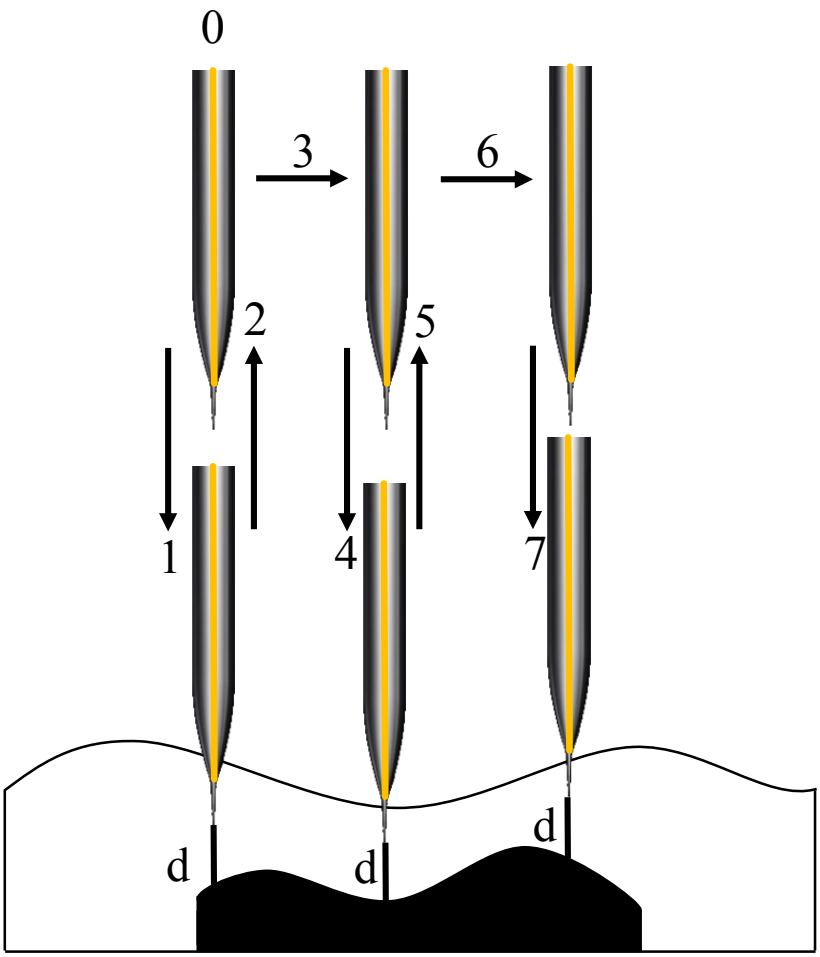

Figure 4: Constant distance schematic. The electrode begins at 0 and is moved sequentially as indicated by the arrows.

To analyze a redox active sample, the working distance can be maintained via Shear Force (SF) microscopy. SF microscopy is implemented simultaneously with SECM and is used to measure morphology and monitor working distance mechanically [13]. SF has the advantage of using the same nanoelectrodes SECM uses, but is unaffected by any chemical reactions taking place in the vicinity of the electrode tip. As shown in Figure 5, piezoelectric wafers are attached to the nanoelectrode, one above the other. The top piezo, the dither, has a high frequency sinusoidal potential applied to excite the nanoelectrode. The vibration of the nanoelectrode results in displacement at the position of the lower piezo, the receiver, which in turn produces a separate potential. As the electrode is lowered toward the sample, the dynamics of the nanoelectrode change

due to the no-slip condition of the fluid at the sample surface. By establishing a voltage threshold similar to the current threshold in constant distance SECM operation, a constant working distance can be maintained to accurately distinguish the current to distance and redox activity [14].

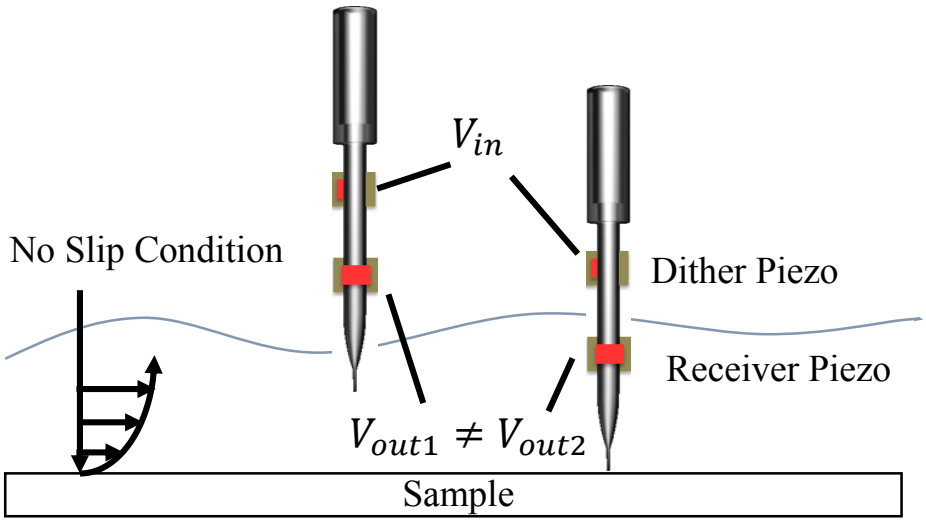

Figure 5: Nanoelectrode with piezoelectric in SF operation [15].

1.2 Identification of the problem

Though the implementation of simultaneous SECM and SF techniques provides a viable solution to the challenges presented by rough surfaces, the technique is still limited. One of the major advantages of SF microscopy is that it can be accomplished using the same nanoelectrodes that have been used for SECM measurement; a characteristic which makes simultaneous SECM and SF possible. However, the SF response obtained from modern SECM electrodes have low amplitude and sensitivity which hinders accuracy when monitoring z-position of the nanoelectrode. SF sensitivity is likely result of the fabrication process and materials which introduce further shortcomings.

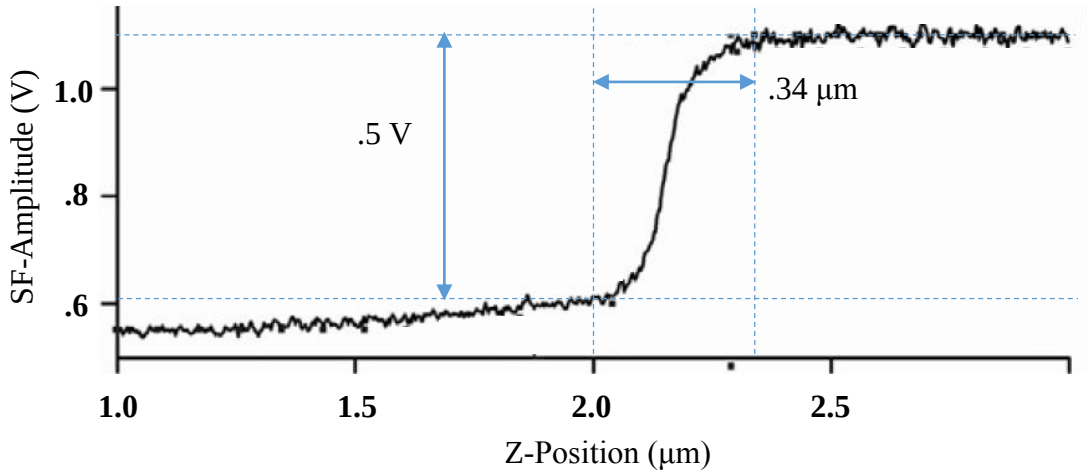

Figure 6: SF Approach

In Figure 6, a SF approach curve is shown which relates z-position of the nanoelectrode to the voltage produced at the receiver [9]. The normalized peak to peak voltage between contact and bulk is only .5 V/V and sensitivity is only 1.5 (V/ µm)/V. In practice, the low amplitude and sensitivity result in greater influence from particulates in solution which is difficult to distinguish from voltage changes due to the boundary layer. Furthermore, poor SF characteristics result in inaccuracies while maintaining the working distance of the electrode. The SF response of the system is contingent on the dynamics of the nanoelectrode itself. Specifically, inherent dampening in the nanoelectrode reduces the influence of the boundary condition on the vibrational amplitude at the receiver. There are several sources of dampening in the system, however most are assumed to be negligible compared to dampening of the nanoelectrode itself (a material property and ultimately a product of the fabrication process).

One process used to fabricate SECM nanoelectrodes was outlined by Mezour et.al. and optimized for SECM application [16]. Electrodes fabricating using this method have demonstrated poor SF sensitivity, likely the result of an annealing process making softer electrodes. Furthermore,

Mezour et. al. reports 100% yield for the process, but in attempts to duplicate these results, the experimental yield was about 10%.

1.3 Approach to the Problem

The purpose of this work was to develop a robust method to produce nanoelectrodes capable of effective simultaneous SECM and SF measurement and to improve the SF dynamics of those electrodes.

The annealed glass that formed the body of previous nanoelectrodes was replaced with brittle quartz capillaries, meant to decrease dampening. Failure mode analysis of the method was then conducted using the new material to determine causes of failure at each step. Based on findings, the previous method was altered to increase process yield and make fabrication more repeatable. The dimensions of the electrode tips produced by the final fabrication process are of interest for future work and were observed.

1.4 Conclusions

This work discusses flaws in the fabrication of SECM nanoelectrodes and ultimately improves upon the process. The most significant flaws are low SF amplitude and sensitivity of the product and poor process yield. To resolve these shortcomings, the material was changed and failure mode analysis was conducted to determine the cause of process failure. Changes were then implemented to the process based on observations which increased process yield to about 58%. Electrodes produced using the new material and process demonstrated SF amplitudes and sensitivities more than twice their predecessors.

The rest of this work is outlined as follows. Chapter 2 focuses on the methods implemented to meet the objectives of this project. Chapter 3 includes all pertinent results of this work including

the final fabrication process and tip dimensions. The final chapter contains conclusions drawn from this work as well as future work to be conducted.

Chapter 2: Methods

This work takes a basic procedure presented by Mezour et. al. and improves its yield by about 580% [16]. Materials used for fabrication play an important role in the fabrication process and are outlined below before the methodology behind alterations are discussed.

2.1 Materials and Tools

Table 1: Fabrication Materials

Quantity	Material	Dimensions/Specs	Vendor
1	Quartz Capillary	I.D.: 5 mm, O.D.: 1 mm, L:10 cm	Sutter Instrument, USA
1	Borosilicate Capillary	I.D.: 1.16 mm, O.D.: 2mm, L: 20 cm	Sutter Instrument, USA
1	Platinum Wire	d: 25 µm, Purity: 99.9%, L: 7-10 cm	Goodfellow, England
1	Silver Ink	65% Silver	Stan Rubinstein Assoc., USA
1	Copper Wire	D: .25 mm, L: Varies	Any
1	D-sub connector pin	O.D.: 1 mm	Radio Shack, USA

A Sutter P-2000 micropipette puller (Sutter Instrument, USA) was used to form and melt glass around a platinum wire before pulling the structure apart to produce nanoscale tips. The puller is typically used for the production of micropipettes. This is achieved by first applying heat to reduce the viscosity of a capillary. Simultaneously, pull bars apply a small force to each end of the glass until a defined rate of separation is achieved. The laser is then turned off, the machine pauses, and a hard pull is executed in which the pull bars apply a significantly larger force to completely split the capillary into two micropipettes with fine tips. The puller has five parameters which can be controlled according to Table 2.

Table 2: P-2000 Parameters

Variable	Function	Range of Values (Unitless)
Heat	Controls laser output power.	550-950 (Recommended for Quartz)
Filament	Controls laser size.	0-5
Velocity	Controls the speed at which Heat is turned off.	1-255
Delay	Controls delay between Heat off and hard pull.	1-255 (128 = No Delay)
Pull	Controls hard pull force.	1-255

2.2 Initial Process

The nanoelectrode tip fabrication technique can be split into four distinct steps: Forming, Insertion, Sealing, and Parting. The Forming step is used to thin the walls of the capillary to form the glass into an hourglass shape; however, it is important that the inner walls do not melt together. In the Insertion step, the capillary is removed from the puller and platinum wire is threaded through the capillary until it is crosses the thinned region. Sealing is the most important step of the process and refers to the process of further heating the thinned region of quartz, melting the glass around the platinum. Finally, the puller is used to execute a hard pull which separates the quartz/platinum rod and yields two nanoelectrode tips. See Figure 7 for a visual representation of the process.

In the Forming step, the quartz capillary is placed in the puller such that the laser heats its center. Each time the capillary is placed in the puller, a vacuum is created inside the capillary using a small air pump. The pump is connected to the capillary via tygon tubes which are pressed over the ends of the capillary. The glass is then thinned using heating/cooling cycles in a one line program shown in Table 3. Each cycle consists of heating for 40 seconds and cooling for 20 seconds. The puller constantly applies a small force to the electrode which tends to pull the glass

apart; however, for this step the pull bars a clamped using butterfly clips to prevent premature separation.

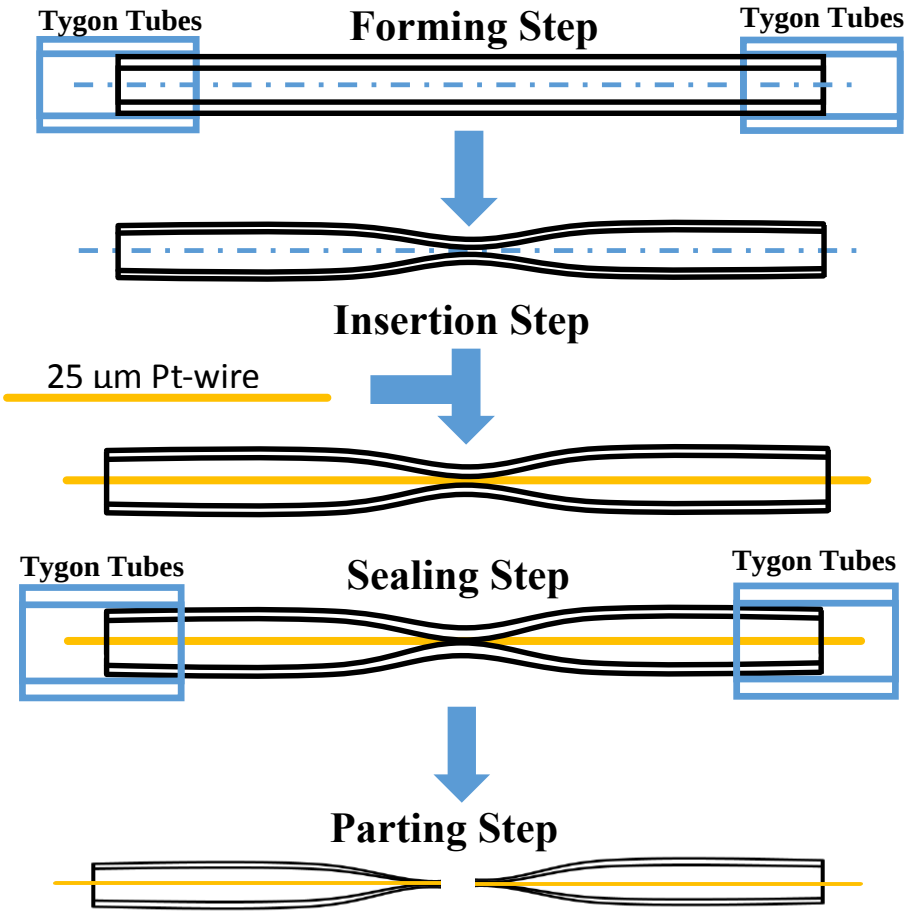

Figure 7: The 4 steps of fabrication of nanoelectrode tips.

Upon completion of the Forming step, the capillary is removed from the puller and platinum is threaded through the glass. The glass is then returned to the puller in exactly the same position as in the Forming step to ensure heating of the same region. Again, tygon tubes are pressed over the capillary ends, a vacuum is created, and the pull bars are restrained. Another single line program, also shown in Table 3, is used to melt the glass around the platinum core. Once the wire is fully sealed in glass, the tubes and pull restraints are removed and the final program is executed. The tip of the pulled electrodes can be checked under a microscope to ensure the platinum is not damaged.

Table 3: P-2000 Programs

Step	Heat	Filament	Velocity	Delay	Pull	Heating Time	# of Cycles
Forming	600	3	N/A	N/A	N/A	40s on/20s off	5
Sealing	540	5	N/A	N/A	N/A	40s on/20s off	5
Parting	780	2	160	100	150	N/A	N/A

Under this regime, there are two important characteristics to note. First, the report states the pump should be left to run for ~30 minutes each time the capillary is placed in the puller. Allegedly this is to ensure a complete vacuum and greater consistency across trials; however, given the size of the capillary and pump capacity, a vacuum can be created in only a few seconds and this recommendation was neglected for the entirety of this work. Second, Mezour's group claims 100% yield for each step except sealing, which yields 60-80% [16]. This means that every time a pull was executed, an undamaged electrode tip was produced. Similar results have not been duplicated by other groups, calling these claims into question.

Nanoelectrode fabrication beyond producing suitable tips is simple. Using an undamaged tip, the end of a ~10 cm copper wire is coated in silver ink and threaded through the open end of the capillary such that it adheres to the platinum core. The protruding end of the copper wire and the back end of the quartz capillary are then inserted into the larger borosilicate capillary until about 1 cm of copper sticks out the end. The remaining centimeter of copper is then coated in silver ink as before and inserted into a D-sub connector pin as shown in Figure 8. In a final step, super glue is applied to the quartz-borosilicate and D-sub- borosilicate joints for stability. The final product is shown in Figure 9.

Figure 8: D-sub pin in borosilicate.

Figure 9: Completed nanoelectrode.

2.3 Failure Mode Analysis

To correct for shortcomings of the fabrication method, the causes of process failure were identified. The thinned region of the pre-pulled electrode and the pulled electrode tip were carefully examined under a microscope after each step to determine modes of failure and in which step they occur. Instances in which an electrode is considered failed are as follows:

- Sealing of the capillary prior to Insertion.
- Melting and separation of the platinum core prior to Parting.
- The platinum wire separates and is not pulled to the end of the tip.
- A gap is present in the wire preventing the flow of current (platinum may still reach the tip).

Steps producing failure were then altered based on observations to reduce process variability and ultimately improve the success rate of each step and overall process yield. The ultimate goal of this project was to improve the process yield beyond 50%.

2.4 SECM/SF Verification and Measurement of Tip Dimensions

After completing the fabrication of nanoelectrodes using the new method, their SECM capabilities were verified via CVs as described in chapter 1. The CVs were conducted in 50 mM ferrocenemethanol solution using an ElProScan system (HEKA, Germany). Potentials ranging from -100-500 mV were applied at the working electrode in three cycles. A Ag/AgCl electrode was used as the reference electrode and a platinum electrode was used as the counter electrode. From each CV the peak to peak current was measured between the fully oxidized and reduced state of the electrode tip. Rearranging equation (1) to solve for the radius of the conducting surface (in this case Pt) yields Equation (2). The theoretical radius of the Pt core is plotted against the measured peak to peak current in Figure 10 [15]. Using Figure 10 the size of the exposed platinum tip was approximated.

$$r_T = \frac{i_T}{gnFDc^*} \tag{2}$$

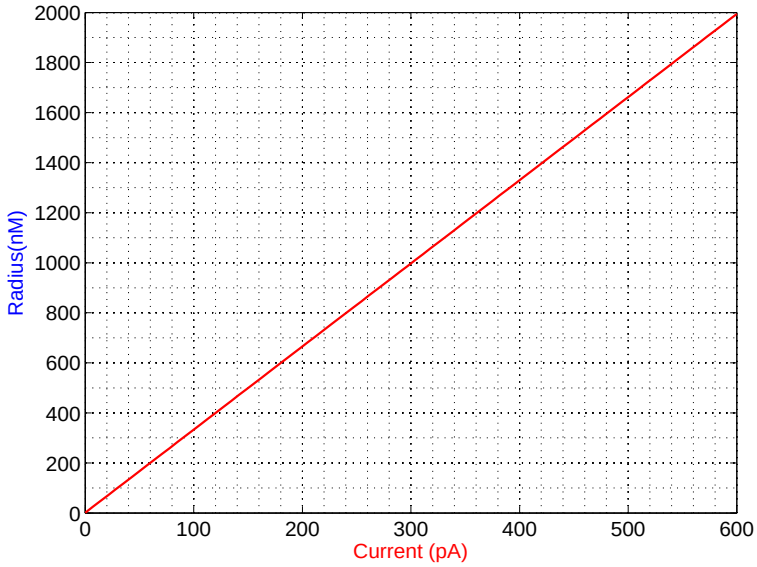

Figure 10: Radius of the conduction portion of an electrode tip vs peak-to-peak current.

Further examination of each electrode was conducted under a microscope to determine other dimensions regarding the tip of the nanoelectrode such as the diameter of the insulating part of the tip, d, and the diameter at the start of the neck, D. The taper length, L, was approximated using a micrometer and the taper angle, θ, was calculated from the other dimensions according to Equation (3). These dimensions are illustrated in Figure 11.

$$\boldsymbol{\theta = \frac{180}{\pi} * sin^{-1}\left(\frac{\frac{D}{2} - \frac{d}{2}}{L}\right)} \tag{3}$$

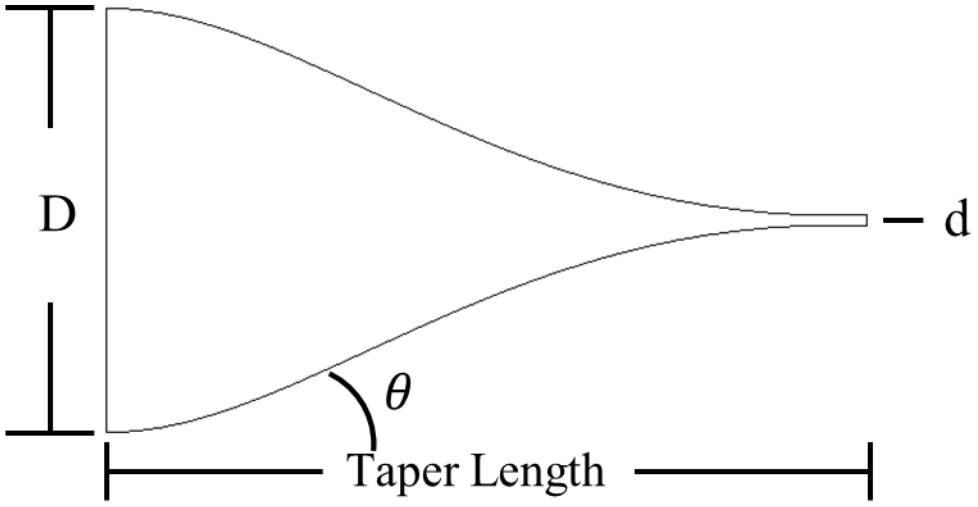

Figure 11: Dimensions of a nanoelectrode tip.

2.5 Conclusions

In this chapter, fabrication materials were identified and a starting point for process improvement was established. The initial process was improved using failure mode analysis with the goal of obtaining 50% yield. After developing an improved process, the dimensions of electrode tips produced using the new method were observed.

Chapter 3: Results

3.1 Failure Modes

Process failure typically refers to the breaking or separation of the platinum core which prevents it from conducting current and ultimately taking electrochemical measurements. This phenomena was a product of the Sealing and Parting steps, however the process can fail before platinum is ever inserted if the inner walls of the capillary melt together preventing insertion as shown in Figure 12. Figure 13 demonstrates a similar mode of failure in which the Platinum is melted in the Sealing step causing it to separate into several beads.

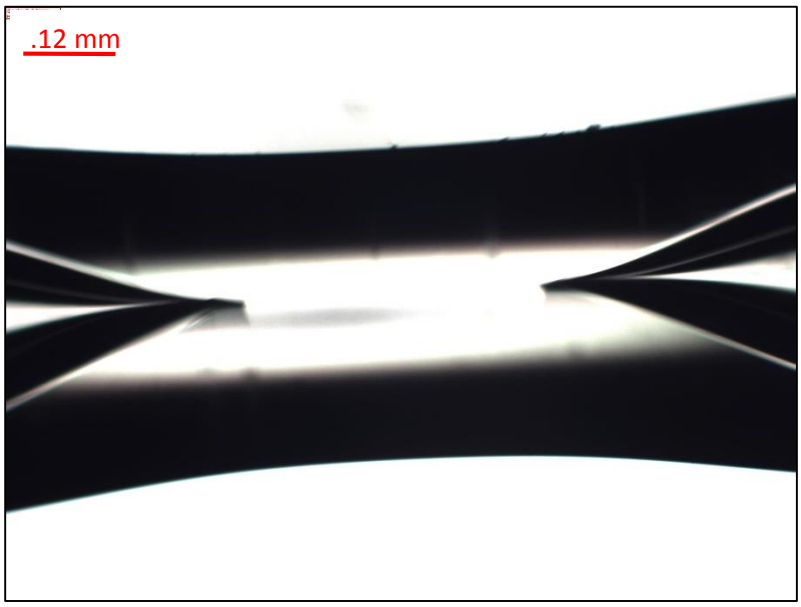

Figure 12: Sealed inner walls.

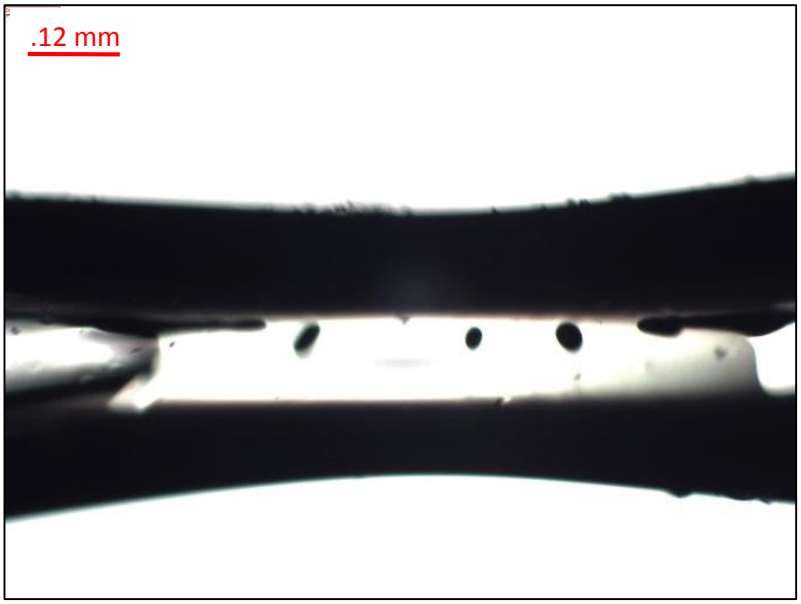

Figure 13: Melted platinum core.

Each of these failures was a result of excessive heating in either the Forming or Sealing step. The remaining types of failure were not directly observed until after the Parting step; however, the Sealing step played a critical role in the success of the pull. Figures 14a and 14b show the same electrode from orthogonal perspectives after the glass has completely sealed around the platinum core. The top view shows that the inner walls of the glass have come together and the

[a]

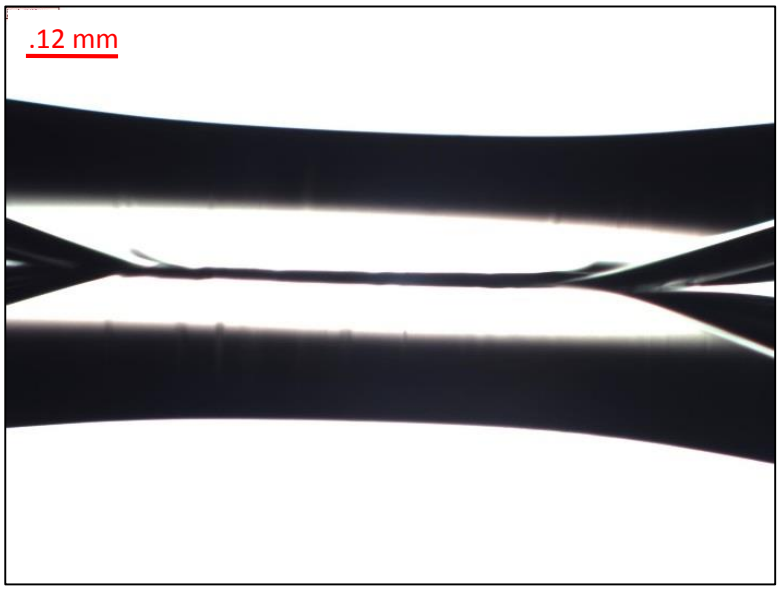

[b]

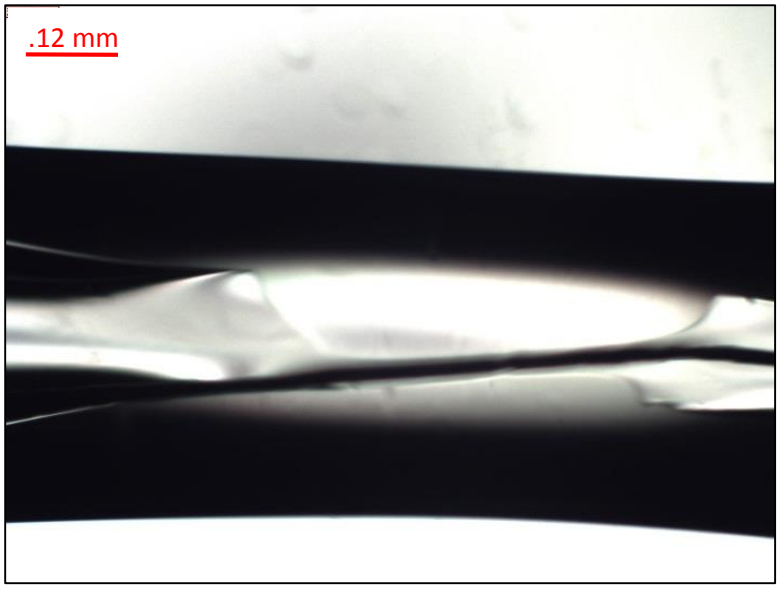

Figure 14: Sealed platinum in one electrode from two perspectives.

platinum bridges the gap, while the bottom view shows how the glass forms around the wire. This is a crucial step in the process, and pull success rates were very low when the glass did not seal properly. A common result, shown in Figure 15, looks like the inner walls have come together but

the glass did not actually sealed around the wire. When pulled, the result was the break shown in Figure 16 where the platinum beaded and terminated in the neck of the electrode tip.

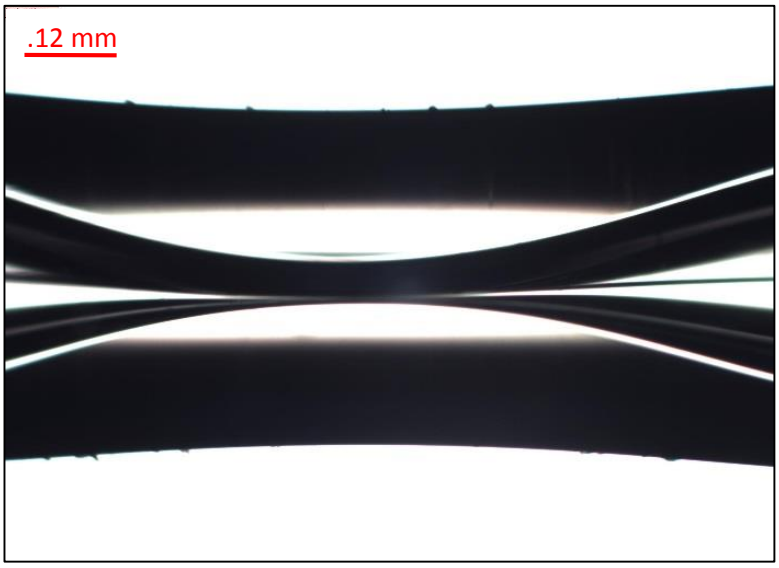

Figure 16: Unsealed Electrode.

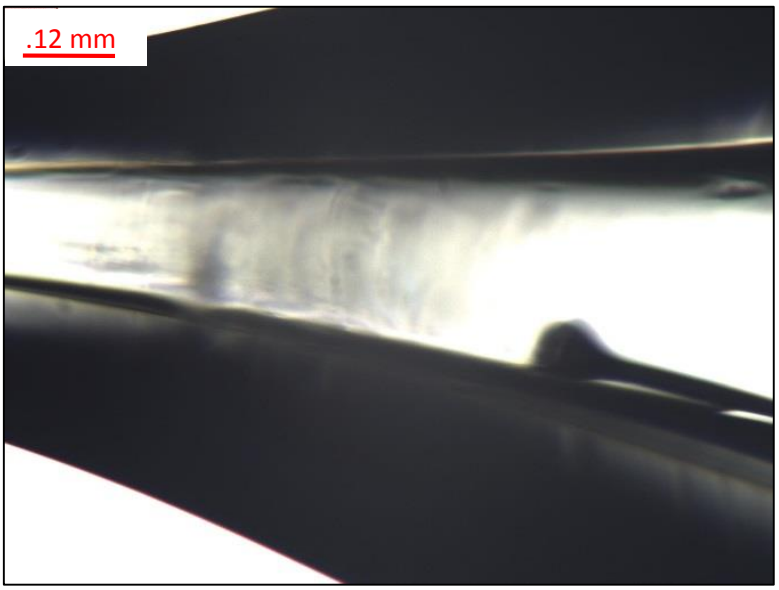

Figure 15: Electrode tip with a break in the platinum which ends in a bead.

If the platinum properly sealed in glass without being damaged, the Parting step also caused damage. If the platinum melted during the pull, it is separated similar to Figure 13 and resulted in the gaps shown in Figures 17 and 18 where there is a gap in the wire but there is also platinum in

the tip. Rather, the glass should be softened more than the wire so it flows around the platinum without actually melting the core. However, the wire was also damaged if the electrode was too hot pulled too hard, resulting in Figure 19. The break was similar to Figure 16, but it occurred past the neck of the electrode.

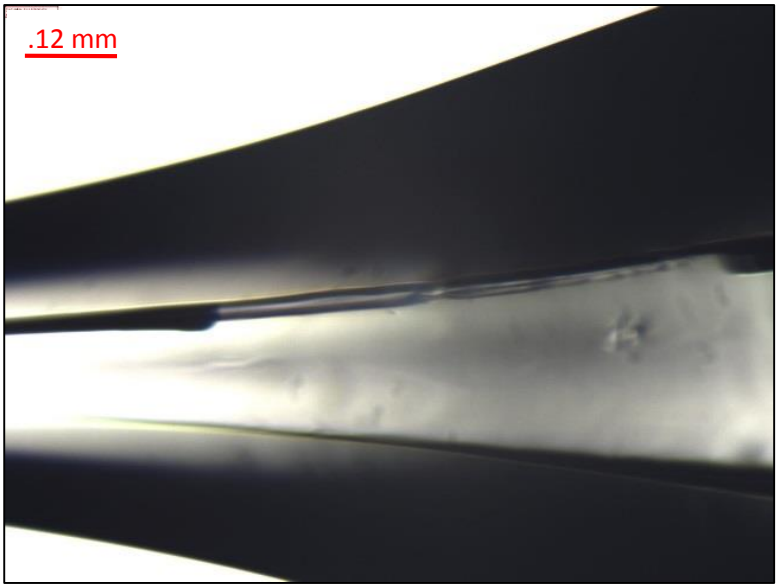

Figure 17: Complete separation of the wire.

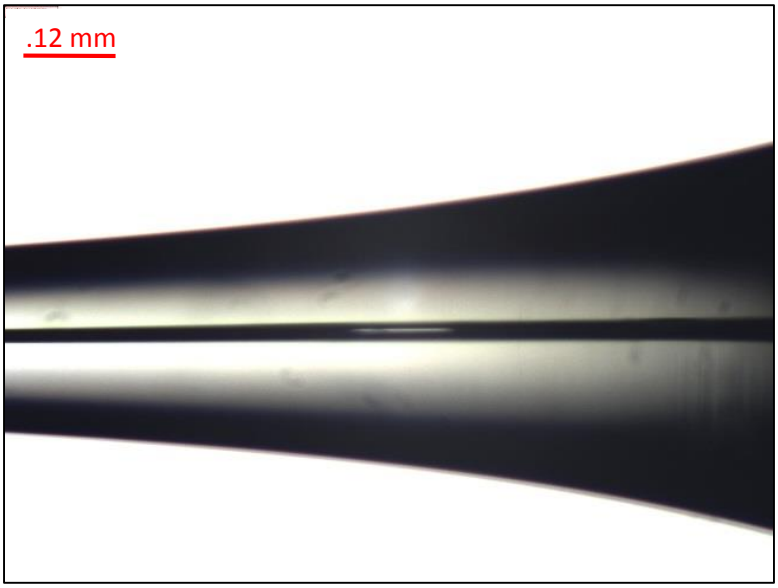

Figure 19: A small gap in the platinum wire.

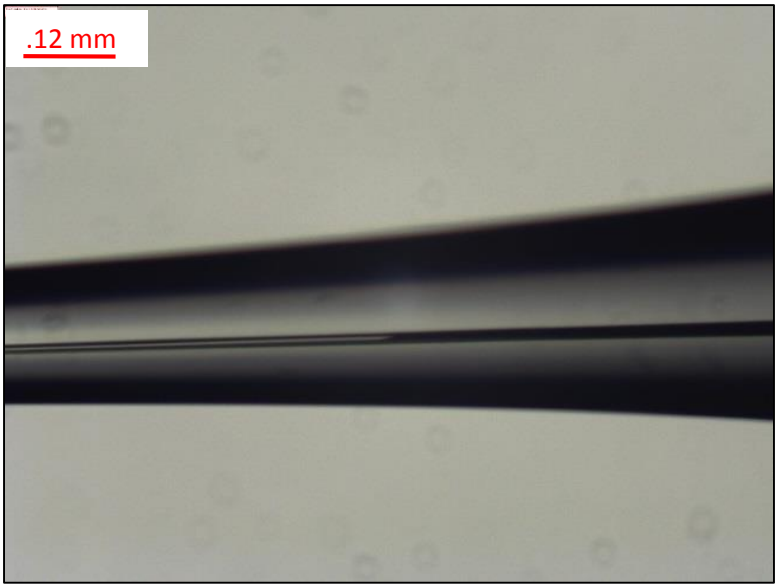

Figure 18: Broken wire past the neck of the electrode.

3.2 Altered Process

Due to the many failure modes outlined above, the fabrication process was altered to reduce the likelihood of those results. The most significant change was to the heating cycle used in the Forming and Sealing steps. Formerly the electrode was heated for 40 seconds and allowed to cool

for 20 seconds each cycle. The result was excessive heating of the platinum which caused melting and separation. To ensure ample cooling time, the cycle was flipped and the electrode was heated for 20 seconds and cooled for 40 which also gave finer control over glass thinning. To compensate for the altered heating cycles (effectively half the heating time) the heat parameter was also changed for each step. The Filament parameter for the Forming and Sealing steps was also made constant for improved consistency. The Heat, Velocity, and Delay parameters for the Parting step were also changed. The Velocity parameter was lowered significantly so the platinum is not as soft during the hard pull and is less prone to separation. A delay of 128 corresponds to no delay between the laser shutting off and the execution of the hard pull. The parameters for each step are shown in Table 4.

Table 4: Adjusted parameters for electrode fabrication.

Step	**Heat**	**Filament**	**Velocity**	**Delay**	**Pull**	**Heating Time**
Forming	700	5	N/A	N/A	N/A	20s on/40s off
Sealing	700	5	N/A	N/A	N/A	20s on/40s off
Parting	745	2	20	128	150	N/A

The number of heating cycles used in the Forming and Sealing steps was also altered. Rather than always running a set number of cycles, a range of an acceptable number of cycles was determined experimentally via the trials outlined in Table 5. For each trial, the parameters in Table 4 were used unless otherwise specified.

Table 5: Record of trials using adjusted parameters. Blue lines indicate successes, white represents failed pulls, and red indicates trials that did not pass the Forming step.

Attempt #	Forming	Sealing	Result
1	8 (heat = 685)	10(heat=685)+6+5	**One success** a beaded break in the other
2	6	6+2	**One success,** complete separation in the other
3	6	8	**One success,** complete separation in the other
4	6	8+4	Gap in one, complete separation in the other
5	7	9+3	**One success,** complete separation in the other
6	8	10	Gap in one, complete separation in the other
7	8	6	Gap in one, complete separation of the other
8	6	8	**One success,** gap in the other one
9	7	---	Capillary sealed before Pt was inserted
10	5	---	Capillary sealed before Pt was inserted
11	4	7	**One success,** complete separation in the other
12	5	---	Capillary sealed before Pt was inserted
13	4+3	6	Good seal, gap in both
14	5	9	**One success,** complete separation in the other
15	6	9	Gap in one, complete separation in the other
16	6	9	Gap in both
17	6	8	**One success,** complete separation in the other
18	6	9+2+2	**One success,** complete separation in the other
19	6	10	**One success,** complete separation in the other
20	6	9	Gap in one, complete separation in the other

Of 17 attempted pulls, 10 were successful and produced tip with no defects giving this process a predicted success rate of about 58.8%: almost 6 times the rate of previous methods. Important to note is that trials 9-13 occurred on the same day and room conditions varied significantly from other days. This indicates that room conditions have an effect on the process and may require that changes be made to P-2000 parameters if this work is repeated. Furthermore, the number of cycles to form was more consistent than the number required to seal. In the Sealing step, the result was specifically meant to match Figure 14, however the result of the Forming step

was less specific. The Forming step was meant to shape the electrode into an hour glass shape that has a gap big enough for the platinum wire to be threaded through. The acceptable range is shown in Figure 20. The spacing in the top image between the two inner walls is about .03 mm and in the

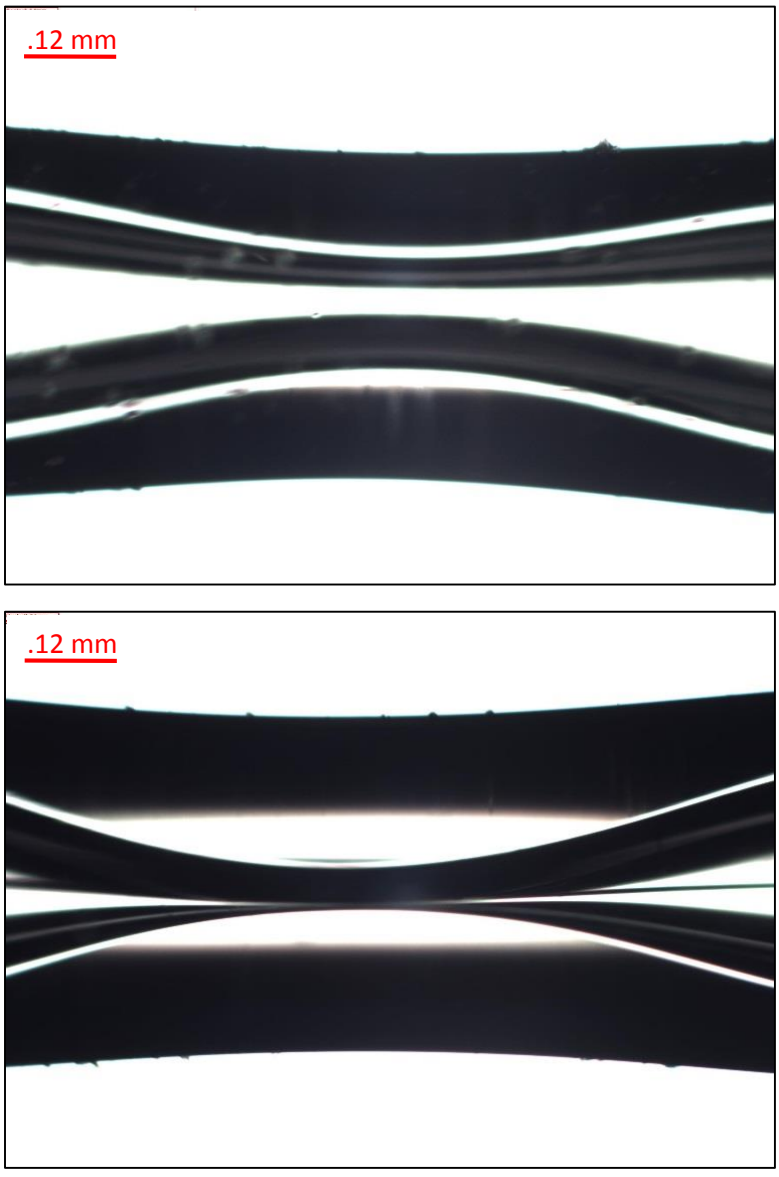

Figure 20: Upper and lower limits for forming glass.

lower image the walls appear to be touching. While glass that has been formed outside this range can work as long as the platinum fits through, this is the guideline based on user experience. Using

these guidelines the results of the number of cycles required for the Forming and Sealing step are shown in Figures 21 and 22.

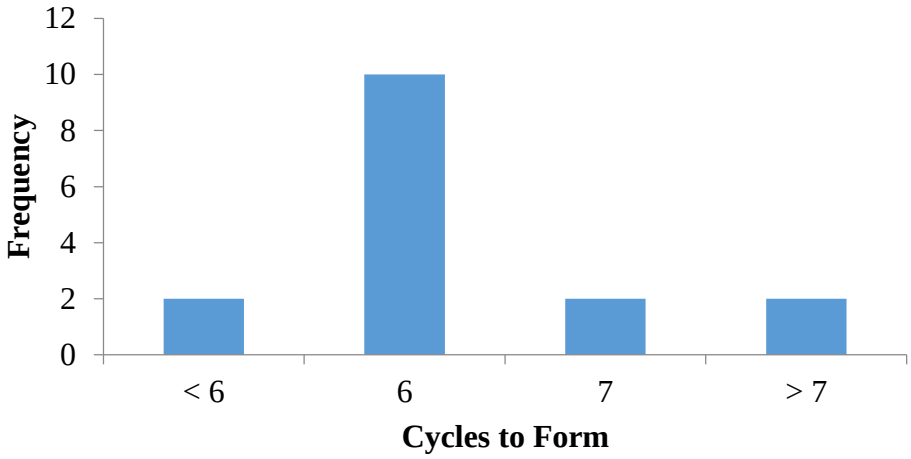

Figure 21: Frequency each number of heating cycles was used to form glass.

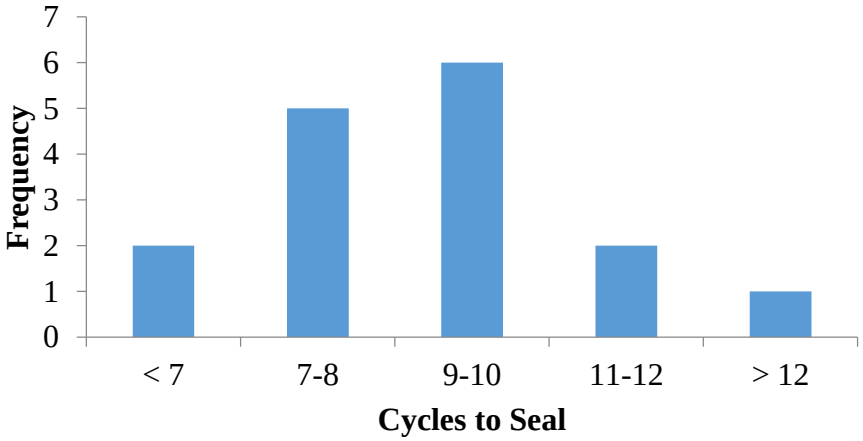

Figure 22: Frequency each number of heating cycles was used to seal platinum in glass.

The most common number of cycles to form was 6 with slight variation around that mode. These variations were likely the result of varying room conditions and operator error. The recommended number of cycles for Forming is 5-8 cycles under the condition that the user check the electrode under a microscope after 5 or 6 cycles to determine if additional cycles are required. Similarly, 7-12 cycles is recommended for Sealing with regular checks after the 7^{th} or 8^{th} to ensure the wire does not melt but is completely sealed in glass. Table 6 illustrates all of the changes made to the process as well as the final fabrication process.

Table 6: Original and adjusted fabrication parameters.

	Forming		**Sealing**		**Parting**	
	Original	**Adjusted**	**Original**	**Adjusted**	**Original**	**Adjusted**
Heat	600	700	540	700	780	745
Filament	3	5	5	5	2	2
Velocity	N/A	N/A	N/A	N/A	160	20
Delay	N/A	N/A	N/A	N/A	100	128
Pull	N/A	N/A	N/A	N/A	150	150
Heat/Cool	40s/20s	20s/40s	40s/20s	20s/40s	N/A	N/A
# of Cycles	5	5-8	5	7-12	1	1

3.3 Electrode Dimensions

Upon successful production of electrode tips, the remainder of the electrodes were assembled according to the procedure outlined in Chapter 2. The dimensions of 7 nanoelectrodes were then observed/calculated. A CV was conducted using each to verify its SECM capability. Furthermore, the peak to peak currents of the CVs were used with Figure 9 to approximate the size of the platinum disk exposed at the tip of each electrode as shown in Figures 23 and 24. CVs of the remaining 6 nanoelectrodes are in Appendix A. The size of the platinum disk and the other tip dimensions discussed in Chapter 2 are presented in Table 7.

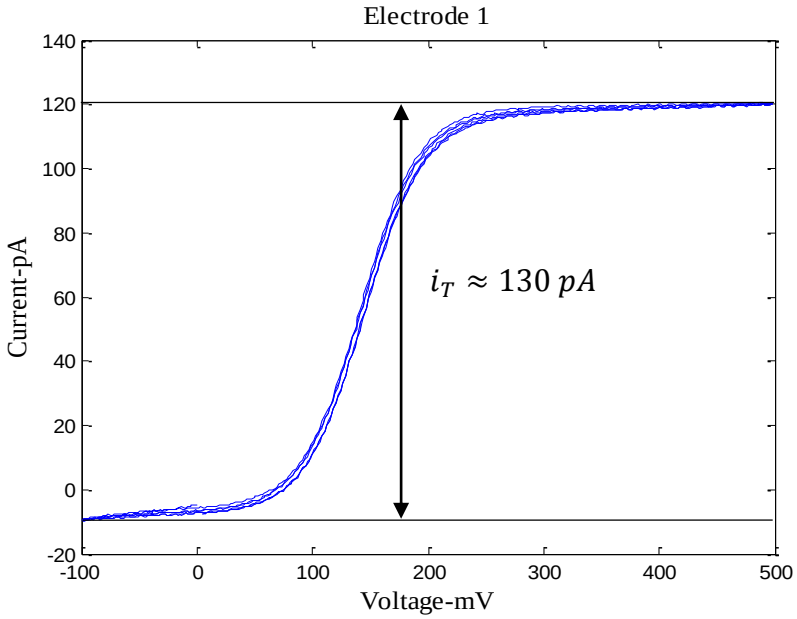

Figure 24: CV of Electrode 1.

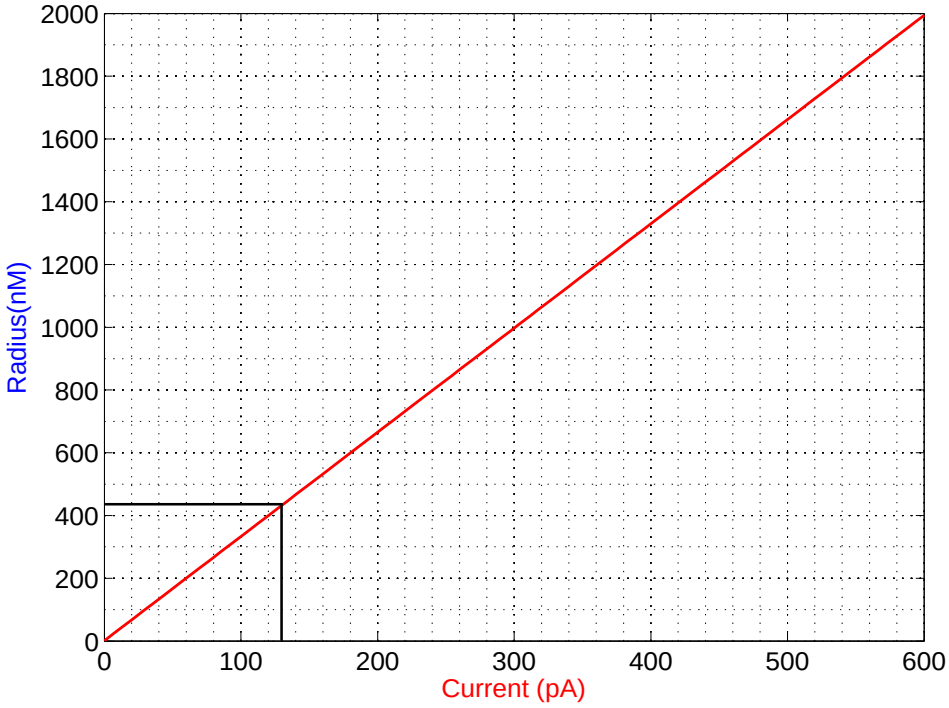

Figure 23: Platinum radius vs measured peak-peak current ($r_T = 420$ nm)

Table 7: Electrode dimensions.

Electrode	Pt Diameter (µm)	Tip Diameter, d (µm)	Diameter, D (µm)	Taper Length (mm)	Taper Angle, θ (deg)
1	0.84	48	844	5.40	4.23
2	0.32	18	671	6.35	2.95
3	0.44	30	744	6.03	3.39
4	0.52	54	875	5.08	4.63
5	0.20	24	847	6.35	3.72
6	0.64	32	835	4.76	4.84
7	0.72	30	844	3.81	6.13

Using the data presented in Table 7, the mean and standard deviation for each dimension was calculated. Since the sample size is low, these calculations alone do not represent the true means and standard deviations of the fabrication process. A 95% confidence interval for each dimension was calculated to predict a range within which the true means might fall. The results of this statistical analysis are shown in Table 8.

Table 8: Statistical Analysis of Tip Dimensions

	Pt Diameter (µm)	Tip Diameter, d (µm)	Diameter, D (µm)	Taper Length (mm)	Taper Angle, θ (deg)
Average	0.53	33.71	808.57	5.40	4.27
Standard Deviation	0.23	12.83	73.25	0.93	1.06
Confidence Interval	0.32 - 0.73	21.85 - 45.58	740.82 - 876.32	4.53 - 6.26	3.29 - 5.25

3.4 Shear Force Microscopy Improvement

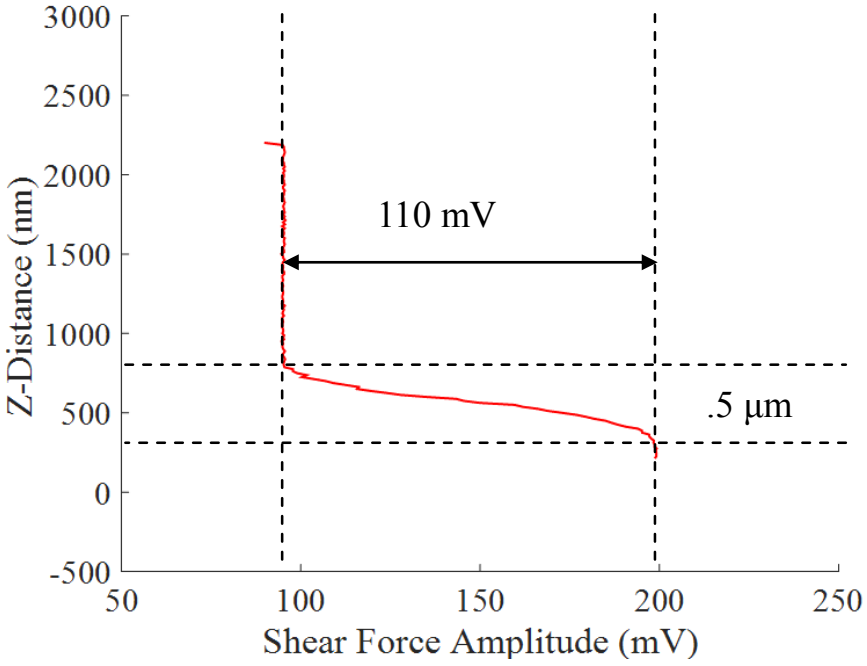

Figure 25: SF approach using a newly fabricated nanoelectrode [15].

After verifying the SECM capability of the newly fabricated nanoelectrodes, the effect of the new process on their SF capability was studied. Using piezo electric wafers as described in Chapter 1, a 100 mV sinusoidal signal was applied to the dither at varying frequencies and the voltage at the receiver was measured as the nanoelectrode was moved toward the surface of a petri dish. A SF approach curve is shown in Figure 25. The normalized amplitude of this curve is about 1.1 V/V and the sensitivity is about 2.2 (V/µm)/V. Similar SF approaches were conducted using electrodes produced by the adjusted fabrication technique outlined by this work for a total of 8 samples [15]. The average amplitude and sensitivity of these approaches were 1.25 V/V and 3.16 (V/µm)/V respectively, more than twice the values calculated for the approach curve in Figure 5 (Amplitude: .5 V/V, Sensitivity: (V/µm)/V). Since the sample size is so low, a 95% confidence interval for both amplitude and sensitivity was calculated and is shown in Table 9. The lower

bounds for each interval also show significant increases in amplitude and sensitivity, indicating a 95% chance of increasing each electrode characteristic on average. Increased amplitude and sensitivity will allow greater control over the position of the electrode tip above a sample surface in practical applications and will ultimately enable more accurate SECM implementation.

Table 9: SF Characteristics of Electrodes Produced Using the Outlined Procedure.

	SF-Amplitude (V/V)	Sensitivity (V/(μm)/V
Average	1.25	3.16
Standard Deviation	.20	1.36
95%Confidence Interval	1.08 – 1.42	1.99 – 4.34

3.5 Conclusions

In this chapter, several failure modes of electrode fabrication were identified. Based on observed failures, the fabrication process was altered resulting in a predicted yield of 58.8%. Electrodes fabricated using the technique outlined in this work demonstrated increases in SF-Amplitude and Sensitivity by 250% and 210% respectively on average. Furthermore, the dimensions of electrode tips were measured for applications in future work.

Chapter 4: Conclusion

In Chapter 1 I identified shortcomings in the capabilities of SECM nanoelectrodes as well as low success rates in the process by which electrodes were produced. In Chapter 2, the previous fabrication method was outlined and failure mode analysis was identified as the procedure used to improve the fabrication process. In Chapter 3, I illustrated the results of conducting failure mode analysis: a new fabrication process which increased yield by about 580% and SF amplitude and sensitivity by 250% and 210% respectively on average. The hypothesis that changing the electrode material would increase SF sensitivity was confirmed and the goal of producing electrodes at above 50% yield was met. In Chapter 4 I discuss my contribution to the field and future steps.

4.1 Contributions and Influence

The purpose of this work was develop a robust method to produce nanoelectrodes capable of simultaneous SECM and SF measurement. Through this work I have outlined a new procedure for the fabrication of SECM nanoelectrodes by conducting a Failure Mode Analysis of previous methods and making alterations according to observations. The procedure is predicted to yield at a rate of 58.8%, approximately 5.88 times that of its predecessor. Furthermore, the process of fabricating SECM electrodes has not been the focus of much study. These preliminary results provide a useful starting point for perfecting the fabrication process and will allow further study of electrodes' influence in SECM experimentation. Additionally, the product of the developed procedure is a nanolectrode of the same current measuring capabilities of previous methods, but with over twice the SF amplitude and sensitivity. Reduced annealing of the glass capillaries used in fabrication was identified as a key step in improving SF characteristics of SECM electrodes.

4.2 Future Work

One of the defining characteristics of a nanoelectrode is the dimensions of its tip. While tip dimensions of the fabricated electrodes were noted, the effects of changing fabrication parameters on tip dimensions were neglected. Further study of how tip dimensions are effected by fabrication parameters could further improve the entire process as well the SF sensitivity of the final product.

Another factor which plays a critical role in SF imaging is the frequency at which the potential is applied to the dither piezo. Theoretically, the optimum applied frequency would be the natural frequency of the electrode being used as it would produce the largest displacement at the receiver. However, determining that frequency experimentally is impractical. In a future study, a theoretical model of a nanoelectrode will be produced to approximate a natural frequency. This model could then be verified by conducting an SF approach using the calculated frequencies and comparing it to other approaches at different frequencies of operation.

References

[1] Wittstock, Gunther, et al. "Scanning electrochemical microscopy for direct imaging of reaction rates." *Angewandte Chemie International Edition* 46.10 (2007): 1584-1617.

[2] Kwok, Juhyoun, Chongmok Lee, and Allen J. Bard. "Scanning Electrochemical Microscopy." *J. Electrochem. Soc* 137.5 (1990).

[3] Bard, Allen J., et al. "Scanning electrochemical microscopy. Introduction and principles." *Analytical Chemistry* 61.2 (1989): 132-138.

[4] Wei, Chang, Allen J. Bard, and Michael V. Mirkin. "Scanning electrochemical microscopy. 31. Application of SECM to the study of charge transfer processes at the liquid/liquid interface." *The Journal of Physical Chemistry* 99.43 (1995): 16033-16042.

[5] Scott, Erik R., Henry S. White, and J. Bradley Phipps. "Iontophoretic transport through porous membranes using scanning electrochemical microscopy: application to in vitro studies of ion fluxes through skin." *Analytical chemistry* 65.11 (1993): 1537-1545.

[6] Kwak, Juhyoun, and Allen J. Bard. "Scanning electrochemical microscopy. Theory of the feedback mode." *Analytical Chemistry* 61.11 (1989): 1221-1227.

[7] Kranz, C., et al. "Imaging of microstructured biochemically active surfaces by means of scanning electrochemical microscopy." *Electrochimica acta* 42.20 (1997): 3105-3111.

[8] Sklyar, Oleg, et al. "Modeling steady-state experiments with a scanning electrochemical microscope involving several independent diffusing species using the boundary element method." *The Journal of Physical Chemistry B* 110.32 (2006): 15869-15877.

[9] Danis, Laurence, et al. "Development of nano-disc electrodes for application as shear force sensitive electrochemical probes." *Electrochimica Acta* 136 (2014): 121-129.

[10] Saito, Y. "A theoretical study on the diffusion current at the stationary electrodes of circular and narrow band types." *Rev. Polarogr* 15 (1968): 177-187.

[11] Kranz, C., et al. "Mapping of enzyme activity by detection of enzymatic products during AFM imaging with integrated SECM–AFM probes." *Ultramicroscopy* 100.3 (2004): 127-134.

[12] Ballesteros Katemann, Bernardo, Albert Schulte, and Wolfgang Schuhmann. "Constant-Distance Mode Scanning Electrochemical Microscopy (SECM)—Part I: Adaptation of a Non-Optical Shear-Force-Based Positioning Mode for SECM Tips." *Chemistry–A European Journal* 9.9 (2003): 2025-2033.

[13] Brunner, R., et al. "Distance control in near-field optical microscopy with piezoelectrical shear-force detection suitable for imaging in liquids." *Review of scientific instruments* 68.4 (1997): 1769-1772.

[14] Ballesteros Katemann, Bernardo, Albert Schulte, and Wolfgang Schuhmann. "Constant-Distance Mode Scanning Electrochemical Microscopy. Part II: High-Resolution SECM Imaging Employing Pt Nanoelectrodes as Miniaturized Scanning Probes." *Electroanalysis* 16.1-2 (2004): 60-65.

[15] Northcutt, Robert G., and Vishnu-Baba Sundaresan. "Mechanoelectrochemistry of PPy (DBS) from correlated characterization of electrochemical response and extensional strain." *Physical Chemistry Chemical Physics* 17.48 (2015): 32268-32275.

[16] Mezour, Mohamed A., Mario Morin, and Janine Mauzeroll. "Fabrication and characterization of laser pulled platinum microelectrodes with controlled geometry." *Analytical chemistry* 83.6 (2011): 2378-2382.

Appendix A

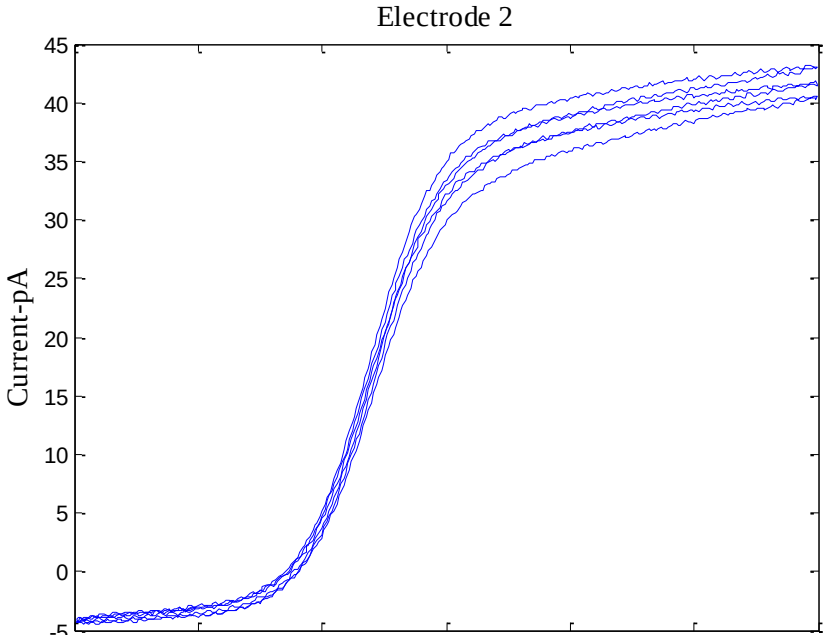

Figure A1: CV of Electrode 2

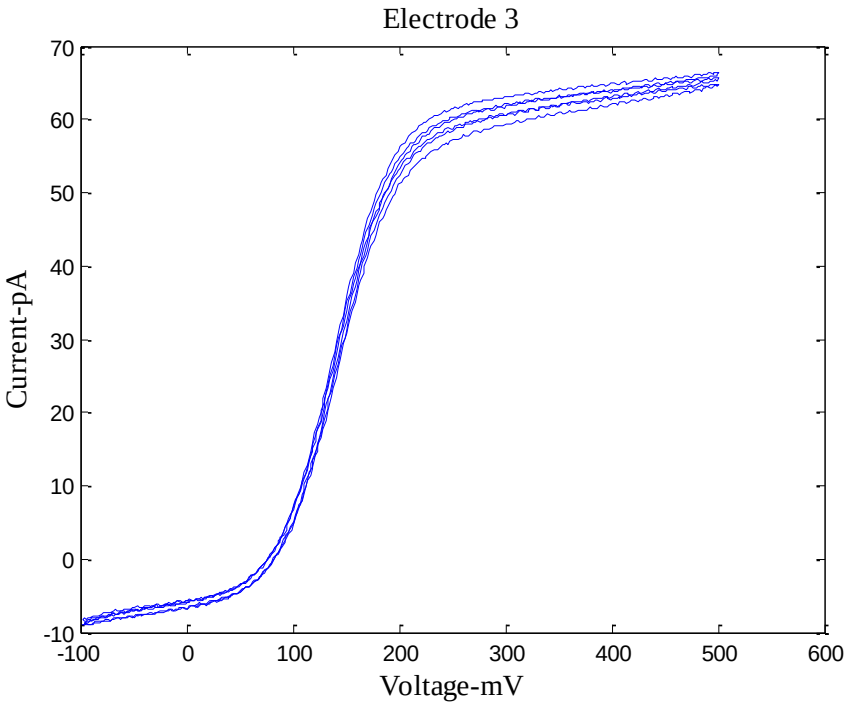

Figure A2: CV of Electrode 3

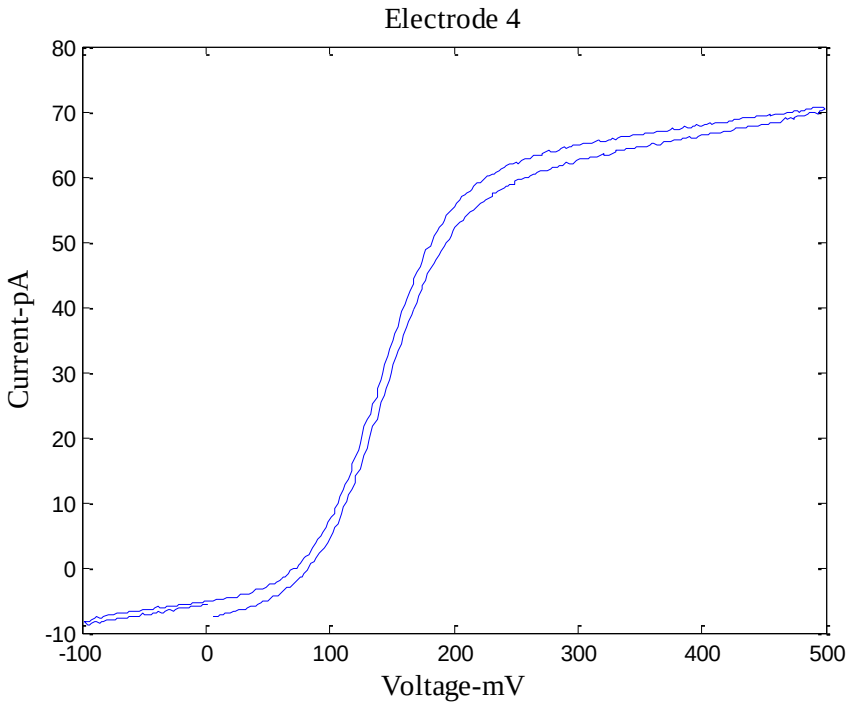

Figure A3: CV of Electrode 4

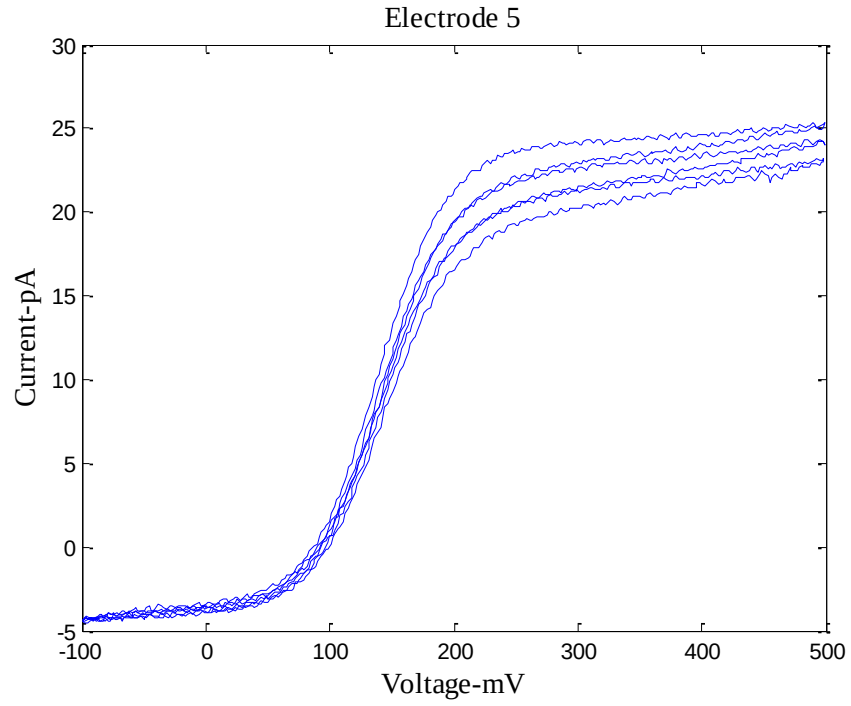

Figure A4: CV of Electrode 5

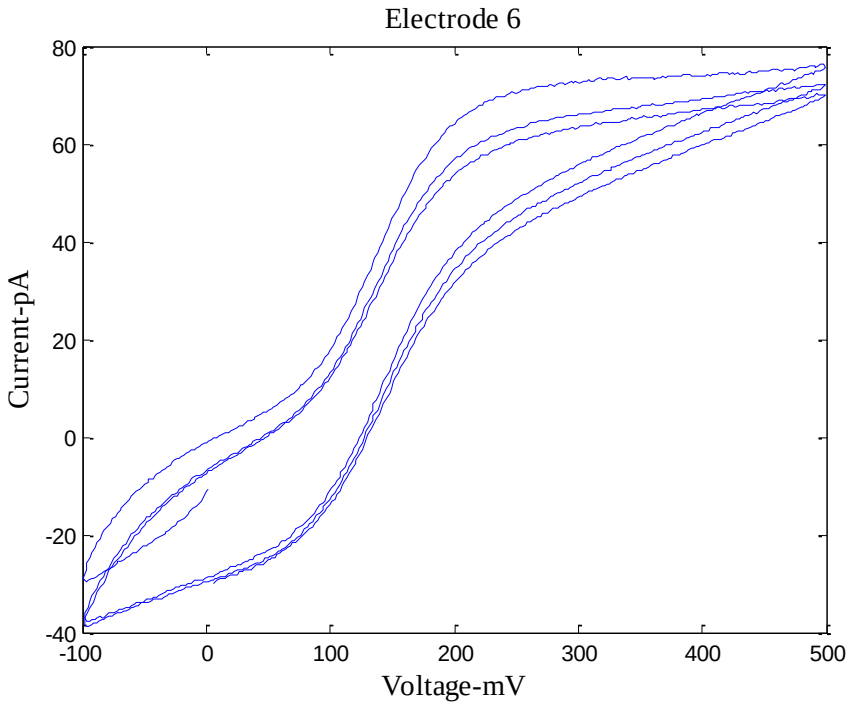

Figure A5: CV of Electrode 6

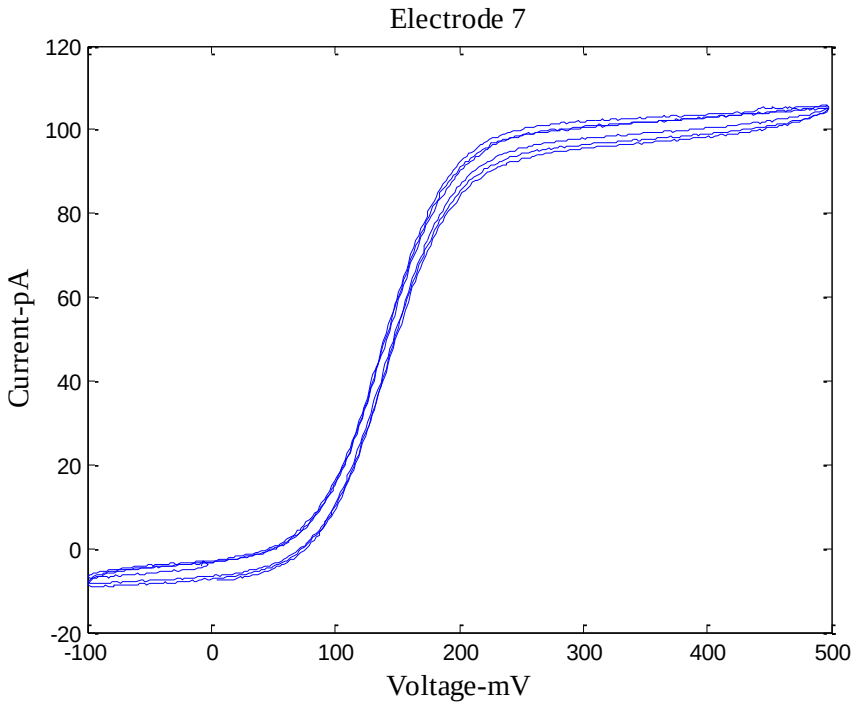

Figure A5: CV of Electrode 7